

# Obtaining AVO and AVA curves from CRS attributes

Ricardo Biloti, Rodrigo Portugal,  
Lúcio T. Santos & Martin Tygel

State University of Campinas

## Abstract

We present a method to obtain amplitude-versus-offset (AVO) and amplitude-versus-angle (AVA) curves at selected depth points using the three attributes generated by the Common Reflection Surface (CRS) stack, the emergence angle and the two hypothetical wavefront curvatures associated to each zero-offset ray simulated. Our approach combines the CRS stack/inversion process applied to multicoverage data and the use of a kinematic Kirchhoff migration to achieve true-amplitudes (TA) at assigned depth points in the migrated images. The proposed method consists of the following steps: (i) apply the CRS process to the given multicoverage data; the obtained CRS attributes are then used to produce a simple macro-velocity depth model; (ii) perform an unweighted Kirchhoff migration for imaging purposes only; for selected points on target reflectors in the migrated image, we use ray tracing within the macro-velocity model to determine, by ray tracing, common-reflection-point (CRP) gathers that belong to the input data; for these rays, we compute the incident angles and the geometrical spreadings; (iii) go back to CRP gathers and compensate the amplitudes for geometrical spreading. The whole process permits to construct AVA curves on the assigned CRP's. In summary, our method is designed to aggregate amplitude information on selected points of a reflector, after a purely kinematic image (migration) has been obtained. The method is tested on a synthetic inhomogeneous layered model with encouraging results.

# Introduction

One of the main objectives of processing seismic reflection data for hydrocarbon prospecting is to obtain meaningful images of the geological structures, in particular reservoir structures in the subsurface. The geological structures to be imaged are defined by seismic reflectors given by interfaces of discontinuity of rock parameters, such as velocity and density.

Kinematic images, in which only the location and orientation of the reflectors (with no regard to amplitudes) are considered, can be achieved, for example, by efficient Kirchhoff migration procedures using simple weights or no weights at all. Kirchhoff migration requires a given macro-velocity model that incorporates in the best possible way the *a priori* information, such as previous knowledge of the geology, information from nearby wells, etc. Moreover, special methods exist to combine the migration output to update the model, so as to refine and improve the image. The final result is in many cases a fairly adequate (kinematic) image of the structures of interest.

The problem that concerns us in this paper is how to aggregate dynamic information (physically meaningful amplitudes) to the obtained image. In fact, the amplitudes are needed essentially on selected points at key interfaces along the extension of the reservoir, where the determination of the angle dependent reflection coefficients is the most desirable information.

According to zero-order ray theory, the amplitude of a primary-reflection event can be described by

$$U = \mathcal{A} \frac{\mathcal{R}}{\mathcal{L}}, \quad (1)$$

where  $\mathcal{R} = \mathcal{R}(\theta)$  is the angle-dependent reflection coefficient of the primary reflection ray, and  $\theta$  is the incidence angle of that ray with respect to the interface normal. The reflection coefficient is the quantity of interest to be estimated from the data. The parameter  $\mathcal{L} = \mathcal{L}(\theta)$  is the angle-dependent geometrical-spreading factor of the reflection ray. It accounts for the amplitude variations due to focusing and defocusing of the energy carried by the ray along its raypath. Amplitudes are generally affected by many factors other than the geometrical spreading. These include, for instance, acquisition footprints, transmission losses across interfaces and attenuation. All those factors combined constitute the overall quantity  $\mathcal{A}$  in equation (1). The estimation of this factor is beyond the scope of this paper.

The geometrical spreading factor  $\mathcal{L}$  is generally considered as one of the major sources of amplitude distortion in the observed data. This is the reason why the term *true amplitude* (TA) is typically attached to a primary-reflection amplitude that has been corrected for geometrical spreading.

In the case of depth migration, the term *true-amplitude* refers to the case in which the migration output equals the observed amplitudes automatically corrected for geometrical spreading (see, e.g., Hubral et al., 1996). Referring to equation (1), the corresponding true amplitude of the primary-reflection would be

$$U_{TA} = \mathcal{A} \mathcal{R}. \quad (2)$$

True-amplitude migration algorithms, such as Kirchhoff weighted diffraction stacks, are designed to assign at each migrated depth point an amplitude that is equal to the original primary-reflection amplitude at reflectors after geometrical-spreading correction. Full true-amplitude algorithms are significantly more expensive and time-consuming than their kinematic unweighted counterparts. As another complication, the accuracy requirements on the macro-velocity depth model are higher for the application of true-amplitude migration than for

purely kinematic migration. The flexibility of using migration outputs to update the velocity model is lost when such a heavy and demanding migration algorithm is applied. As the last and probably best argument against the application of a full true-amplitude migration algorithm to an overall region is that, in fact, the amplitude information is required only on some specific target points or reflectors. Away from these points, the obtained amplitudes are not useful.

In this paper, we propose a method to aggregate true amplitudes (i.e., observed primary-reflection amplitudes after geometrical-spreading correction, by means of AVO/AVA curves) at selected CRP's of interest, after an image of the subsurface has been obtained. This image can be, for example, the result of one or several kinematic migrations.

In the next section, we provide an overall description of the proposed approach. We show with the help of a fluxogram the general strategy of the method. Thereafter, we briefly review the fundamentals of the CRS method, in particular the meaning of the CRS attributes. Next, we indicate how the attributes can be used to construct a macro-velocity depth model. This model is used not only for imaging through kinematic migration but also for the construction of CRP gathers on specified depth points. The macro-velocity model is also used to compute the geometrical-spreading factors and incidence angles for all primary-reflection rays that comprise the CRP gathers. Finally, we explain how the geometrical-spreading corrections are applied to the input data, leading to the sought-for AVA curves.

## Strategy

The structure of the method is summarized by the fluxogram shown in Figure 1. Our strategy is mainly divided into three processes: (i) CRS attribute extraction & macro-model inversion, (ii) kinematic imaging through unweighted Kirchhoff migrations, and (iii) subsequent geometrical-spreading corrections to the amplitude of the input data for the selected points.

## CRS stack

The 2-D Common Reflection Surface (CRS) stack (see, e.g., Müller, 1999) applied to multi-coverage data on a seismic line is designed to produce a stacked section (an approximation of a zero-offset section) together with three auxiliary sections of CRS attributes and a coherence section. To be applied, the CRS method requires the knowledge of the near-surface velocity distribution only.

For each fixed central point (e.g., a CMP location of the original data) on which the output trace is to be computed, the CRS stack uses a multiparametric hyperbolic traveltime formula to stack all data that correspond to arbitrary source and receiver locations in the vicinity of that point. In this sense, it differs significantly from the conventional NMO/DMO/stack (that employs only reflections from CMP gathers) to achieve much more redundancy with a consequent improvement of signal-to-noise ratio. The three CRS attributes assigned to each point of the stacked section are the parameters of the traveltime moveout formula. These are the emergence angle of the normal reflection ray and the wavefront curvatures of the normal-incidence-point (NIP) and normal (N) waves arriving at that point.

The N- and NIP-waves are fictitious eigenwaves introduced by Hubral (1983) for the analysis of the actual propagation of the zero-offset ray, as well as for its corresponding paraxial rays. Their wavefront curvatures at the central point carry important information about the velocity

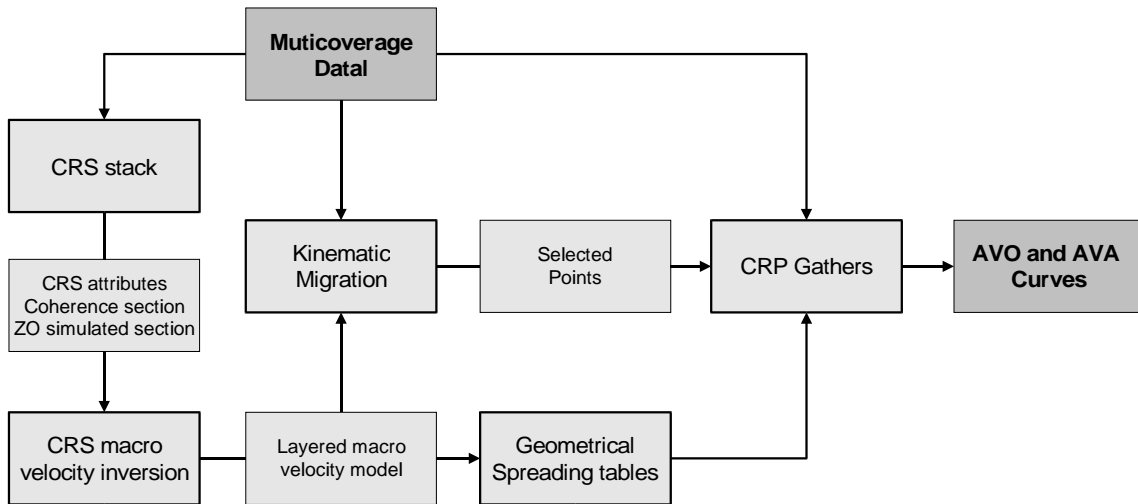


Figure 1: Flowchart of the method: The CRS stack method is applied to the multicoverage data to obtain the CRS attributes, that are subsequent used as input for the CRS inversion. The obtained velocity model is then used by the kinematic migration algorithm. After migrating all common-offset sections of the multicoverage data and stacking them to build a kinematic image, we can easily selected interested points to analyse, by means of AVO/AVA curves. Using the information in the geometrical-spreading factor tables, namely traveltimes and reflection point positions, the CRP gathers are extracted from the multicoverage data. Finally, picking the interested amplitude, the geometrical-spreading correction is applied to build up the AVO/AVA curves.

model in which the wave propagation takes place. The N-wave can be conceptually visualized as the one that starts as a wavefront that coincides with the reflector and travels to the surface with half of the medium velocity. It arrives at the central point at the same time as the zero-offset ray. The NIP-wave can be visualized as starting as a point source at the reflection point of the zero-offset reflection ray and propagates upwards with half of the medium velocity. It arrives at the central point at the same time as the zero-offset ray, too.

The CRS attributes are extracted upon the use of a coherency analysis strategy directly applied to the data. The development of more efficient and accurate parameter extraction methods is a topic of active research (see, e.g. Birgin *et al.*, 1999).

## Macro-velocity model inversion

The philosophy of the CRS method is to use as much data as possible during the stacking process. Therefore, the most relevant events are well defined on the stacked section and available for further inversion.

The input data for the CRS macro-velocity model inversion are the CRS attributes related to selected target reflections. Also, the near-surface velocity field needs to be known. In fact, this is already a requirement for the application of the CRS stack method.

The classical layer-stripping velocity inversion algorithm of Hubral and Krey (1980) can be recast in terms of the CRS attributes. We have developed an improved process that inverts the selected time reflections to corresponding interface positions together with layer velocities in

depth. The interfaces are constructed as cubic splines, adjusted in a least squares sense, which are suitable for further blocky ray tracing algorithms. Currently, only homogeneous layers can be recovered by the method. This limitation is under active research. An extensive description of this method will be published in a separate paper.

## Kinematic image

Once the homogeneous layered velocity model is provided by the CRS inversion, it is smoothed in order to perform a kinematic migration. The traveltimes tables are generated “on the fly” by the wavefront construction method, and therefore seismic traces can be migrated independently from each other. To enhance the signal-to-noise ratio, the final image is built by stacking all common-offset migrated sections.

## Geometrical-Spreading Correction

On the stacked migrated section, it is possible to choose depth points on a target reflector. For each chosen point, we compute traveltimes, incident angles, and geometrical-spreading factors, by standard dynamic ray-tracing, using the inverted homogeneous layered model. These quantities enable one to extract a CRP gather from the original data.

For each trace, we pick the amplitude, using the computed reflection traveltimes, and multiply it by the corresponding geometrical-spreading factor. A successive application of the procedure to all traces in the CRP gather leads to the desired AVO/AVA curves.

## Numerical examples

The synthetic model, depicted in Figure 2, is composed by four layers separated by smooth interfaces. The first and fourth layers are homogeneous with constant compressional velocity of 2.0 km/s and 2.7 km/s, respectively. The second and the third layers are inhomogeneous. Their velocities are linear combinations of the velocities just below the upper interface and the velocity just above the lower interface of the layer. In other words, these interfaces can be seen as isovelocities lines, implying a variation on the velocity not only in the  $z$ -direction, but also in the  $x$ -direction. For those layers, the compressional velocity varies from 2.2 km/s to 2.4 km/s and from 2.5 km/s to 2.55 km/s, respectively. The shear velocity in each point of the model has been set equal to the compressional velocity divided by  $\sqrt{3}$ . The density is unitary in the whole model.

The synthetic data was modeled by elastic ray tracing. The multicoverage data is composed by 501 common-shot (CS) experiments where the sources are 20 m spaced. Each CS section has 151 receivers, 20 m spaced. The signal-to-noise ratio in the data is 7:1. Figure 3 shows a typical common-offset section. Each common-offset section was migrated separately. All the migrated sections were then summed up to generate the stacked migrated section of Figure 3. The velocity model employed on the migration process (see Figure 4) was obtained from the CRS attributes by the inversion process briefly described above. Note that the inverted model consists of a “best possible” homogeneous layers only, since each layer velocity was recovered as a mean of the actual layer velocity distribution, in a least square sense.

Since the migration was carried out with a reasonable approximated model and several common-offset migrated section were stacked, the obtained stacked migrated section provides

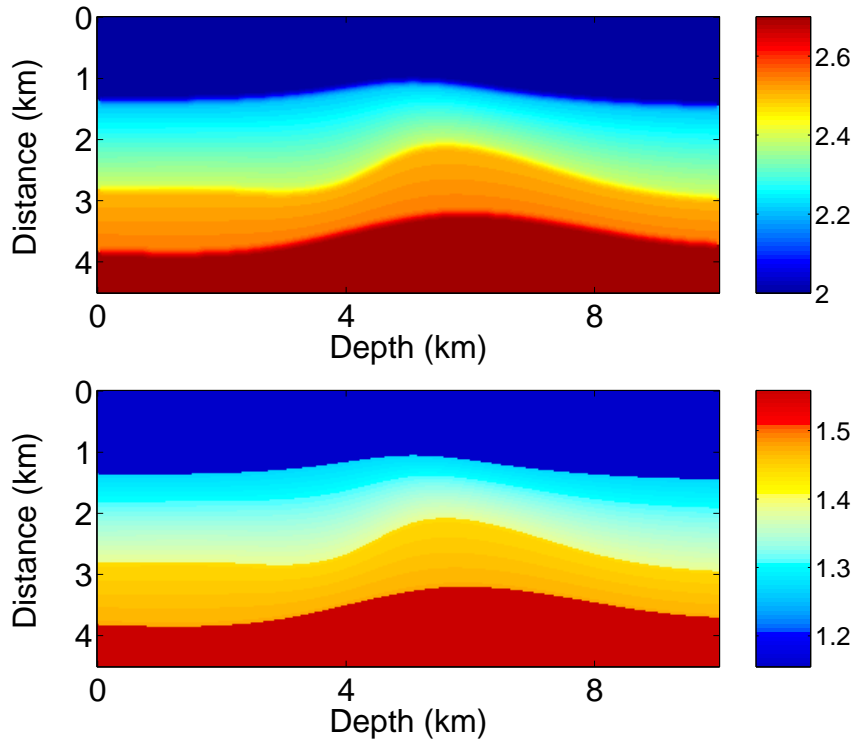


Figure 2: Velocity model for synthetic data. Top: compressional wave velocity map. Bottom: shear wave velocity map.

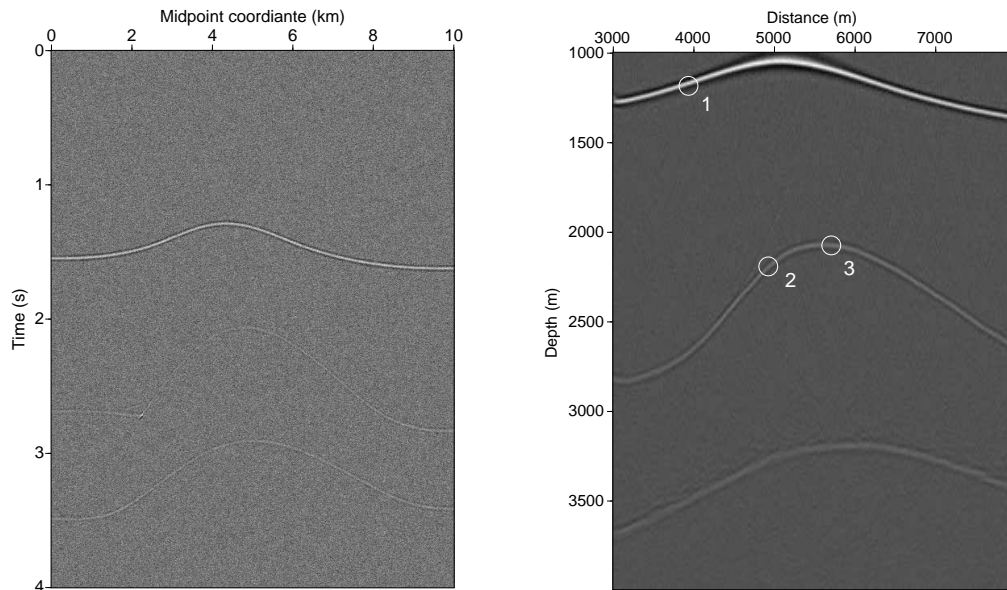


Figure 3: Left: A typical common-offset section for the offset 1500 m. Right: Stacked migrated section. The white circles show the three selected points that are further analyzed.

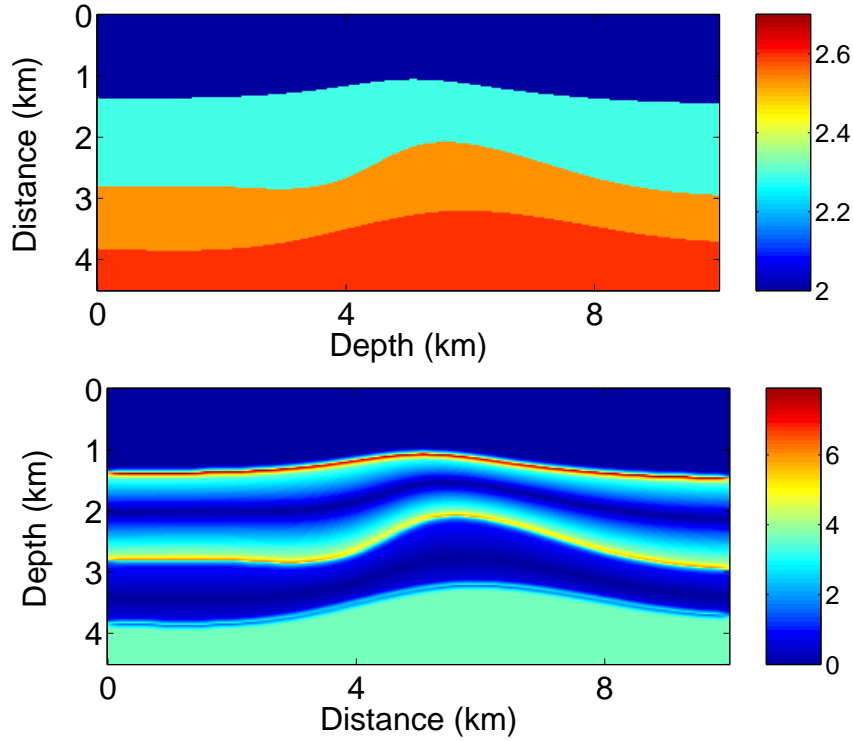


Figure 4: Top: Compressional velocity model obtained by the CRS inversion algorithm. Bottom: Percentual relative error between the real and the inverted model.

an accurate kinematic image in depth. Using this image, we can select points on target reflectors for which AVO/AVA curves are desired. We have chosen three points: one is located at the first interface and two at the second interface (see Figure 3). For each point, we have constructed by forward modeling (on the inverted model) the corresponding CRP section. This means that the traveltime, the reflection angle and the geometrical-spreading factor for each ray of the CRP gather are known. This information is used to pick and correct the amplitudes of the reflection events within the input data.

Figure 5 shows the CRP section associated with the first selected point, located at the first interface. The white strip indicates the region around the traveltime computed by modeling, along which we have performed the amplitude picking. The picked amplitudes are corrected by multiplying them by the geometrical-spreading factor computed by modeling on the inverted model. When plotting the corrected amplitudes versus offset, we generate the AVO curve depicted in Figure 5 (top right). The blue crosses are the corrected amplitudes normalized by the corrected amplitude of the first trace and the solid red line is the correct (modeled) normalized reflection coefficient. Note that, due to the very accurate matching, it is quite difficult to see the red curve. When we plot the same amplitudes versus the reflection angle (computed by modeling), we generate the AVA curve depicted in Figure 5 (bottom right). The same good adjustment can be seen. Figures 6 and 7 show the CRP section and the AVO/AVA curves for the two selected points at the second interface. The second point is located at the top of the dome structure. The computed traveltime is again very precise. The blue crosses in both AVO/AVA curves, depicted in Figure 6 (right), are well distributed around the true normalized reflection coefficient. The same behavior can be observed in Figure 7, for the third selected

point, located at the left flank of the dome structure. Note that the signal-to-noisy ratio of 7:1 is much more problematic for deeper events, since their amplitudes are more attenuated.

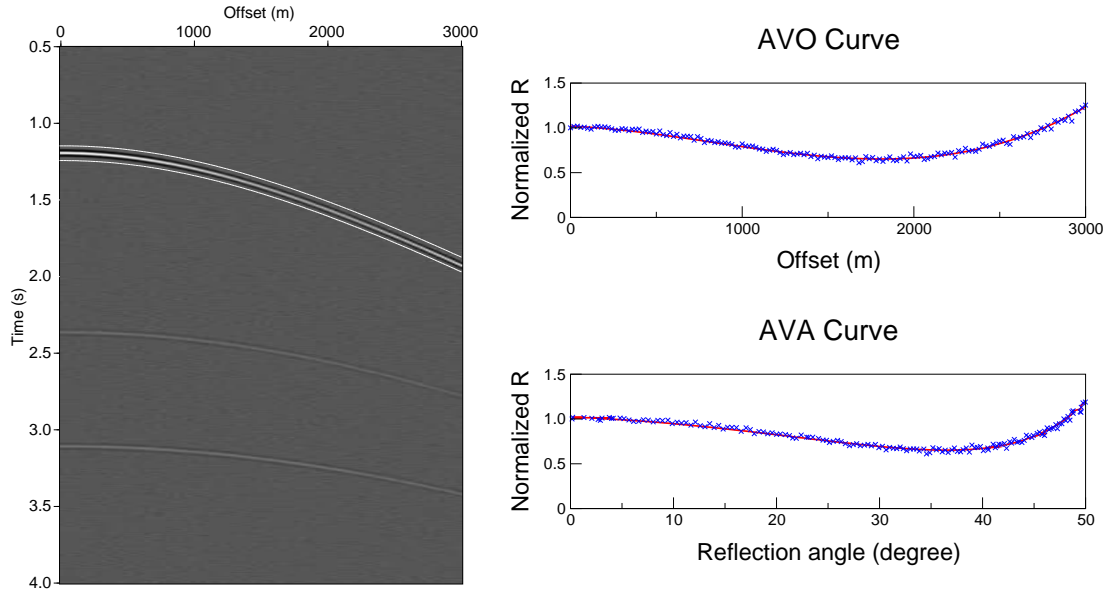


Figure 5: Point 1 on the first interface. Left: CRP section. The white strip confines the region where the picking process was carried out. This region was determined by the traveltime estimation that came out of the modeling process. Right: AVO and AVA curves (picked amplitudes, normalized by the amplitude of the first trace, versus offset and reflection angle, respectively).

## Conclusions

We have presented a method that provides a complete process to obtain correct amplitude curves for chosen points on target interfaces. It consists of three steps: (i) construction of a layered macro-velocity model by using CRS attributes (obtained from the multicoverage data); (ii) kinematic migration of data using that macro-velocity model; (iii) *a posteriori* correction for selected points on the migrated section (using traveltime, reflection angle and geometrical-spreading factor computed on the approximated model) with subsequent estimation of AVO/AVA curves. The numerical results are encouraging, concerning accuracy and computational effort. As a next step, further tests in real data will be carried out.

## Acknowledgments

This work was partially supported by Research Foundation of the State of São Paulo (FAPESP) (Grants 97/12125-8 and 97/12318-0) and by the sponsors of the Wave Inversion Technology (WIT) Consortium.



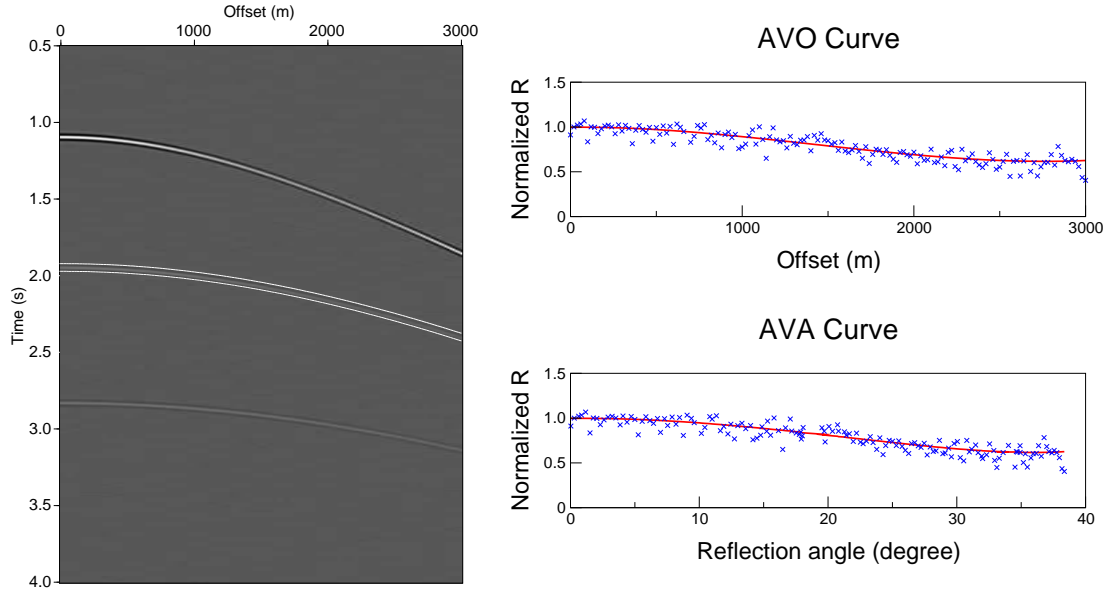


Figure 6: Point 2 on the second interface. Left: CRP section. The white strip confines the region where the picking process was carried out. This region was determined by the traveltime estimation that came out of the modeling process. Right: AVO and AVA curves).

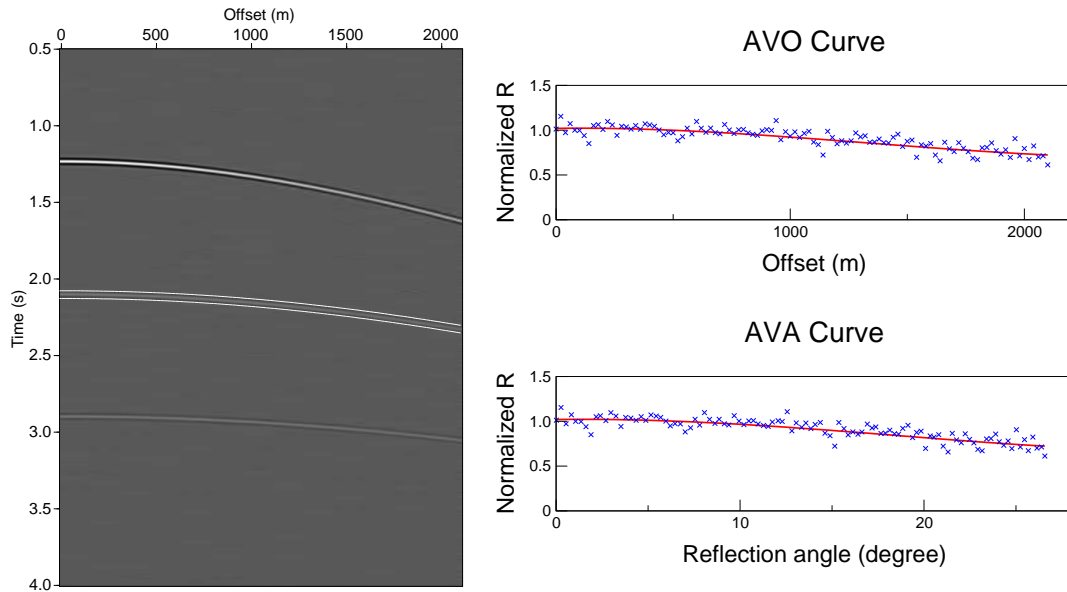


Figure 7: Point 3 on the second interface. Left: CRP section. The white strip confines the region where the picking process was carried out. This region was determined by the traveltime estimation that came out of the modeling process. Right: AVO and AVA curves (picked amplitudes, normalized by the amplitude of the first trace, versus offset and reflection angle, respectively).

## References

- [1] E. G. Birgin, R. Biloti, M. Tygel, and L. T. Santos. Restricted optimization: a clue to a fast and accurate implementation of the common reflection surface method. *Journal of Applied Geophysics*, 42:143–155, 1999.
- [2] P. Hubral. Computing true amplitude reflections in a laterally inhomogeneous earth. *Geophysics*, 48(08):1051–1062, 1983.
- [3] P. Hubral, J. Schleicher, and M. Tygel. A unified approach to 3-D seismic reflection imaging, Part I: Basic concepts. *Geophysics*, 61(03):742–758, 1996.
- [4] Peter Hubral and Theodore Krey. *Interval velocities from seismic reflection time measurements*. Soc. of Expl. Geophys., 1980.
- [5] T. Müller. *Common Reflection Surface Stack Method: Seismic imaging without explicit knowledge of the velocity model*. PhD thesis, Geophysical Institute, Karlsruhe University, Germany, 1999.